Project	ICESTARS
Project Number	FP7/2008/ICT/214911
Work Package	WP3
Tasks	T3.2 and T3.3
Deliverable	D3.6 - extracted document

title	Public report on the implementation of the RF boundary conditions and the transient simulation with adaptive computing facilities
authors	Wim Schoenmaker*, Peter Meuris Monica Selva Soto Sascha Baumanns, Michael Matthes Caren Tischendorf
Corresponding author:	wim.schoenmaker@magwel.com
Affliations	MAGWEL University of Cologne
date	September 30, 2010

Public report on the implementation of the RF boundary conditions and the transient simulation with adaptive computing facilities

Wim Schoenmaker, Peter Meuris
(MAGWEL)

Monica Selva Soto
Sascha Baumanns, Michael Matthes
Caren Tischendorf
(University of Cologne)

September 30, 2010

Contents

1 Introduction

This document describes the mathematical approach that was selected for the activities in WP3 of ICESTARS. In order to support compact model building, we need ab-initio field solving to verify / falsify approximations that are made, while building the compact models. Whereas in the frequency domain, a compact modeling procedure was developed in the projects CODESTAR and CHAMELEON-RF, such a procedure was not yet successfully implemented in the time domain. The main stumbling block is the so called Courant limit[1] which requires unrealistically small time steps for progressing in time.

In the underlying work, the transient regime is addressed by implicit methods. This means that a time step is integrated using both the end-point as well as the begin point of the time interval. Our method is inspired by the transient simulation technique which is used in Technology Computer Aided Design (TCAD). In particular, the backward finite difference is leading to a rather enhanced time-step size.

The following topics will be discussed

- The electrical scalar potential V and the magnetic vector potential $\mathbf{A}$. The computation of $\mathbf{A}$ is complicated by the singular character of the equation for $\mathbf{A}$, leading to the requirement of a gauge condition.
- The discretization scheme demands that variables are placed on grid entities. Here, we present the method that the following grid entities contain fundamental variables: nodes contain the scalar potential V, and the semiconductor variables p, n or ϕ_p, ϕ_n. The links contain the fundamental variable $A = \mathbf{A} \cdot \mathbf{n}$, that means A is the projection of the vector potential along the link direction $\mathbf{n}$.
- The ports of the simulation structure, are excited by circuits. Therefore, the set of all equations for the field system is extended with a set of equations that control the port conditions or boundary conditions.
- The material interface conditions must be analysed in the time domain.

The following risks were identified:

- Can we stay consistent with causality requirements?
- Is the final system of linear equations solvable by iterative methods ?

A first technical approach consists of the following scheme. Using the MAGWEL solver, the matrices for the the system-state equations are exported. This system is extended with the circuit equations and the combined system is solved. Of particular interest is the feed-back loop. We consider first field systems that are linear in the time-differential operator. That means that a single system dump suffices for addressing the combined field-circuit problem. After having this problem settled, the more generic approach will be addressed where variables depend in a non-linear way on the state variables. These cases occur when semi-conductors are present.

We have found that both risks as listed above could be adequatly annihilated. By carefully analyzing the electro-magnetic drift-diffusion system of equations we could formulate a system

[1] condition for convergence while solving certain PDEs numerically, arises when using explicit time-stepping methods.

of equations that respects causality requirements. An important ingredient was to introduce an additional variable, the pseudo canonical momentum of the electro-magnetic field. Another important ingredient towards a stable formulation was to consider the gauge condition as an integral part of the system of equations. In this way, redundancy and ambiguity was avoided and as a consequence the resulting linear systems are regular. Of course, these considerations work all in conjunction with the geometrical discretization approach that is pursued in the MAGWEL solvers. As a consequence, the regular nature of the matrices also results into a successful application of iterative solvers.

2 Goals

The goal of WP3 has been to give accurate simulation support to the model developers in WP1 and WP2 concerning device behavior in the transient regime. Whereas the frequency regime has already been developed in a rather advanced stage in earlier projects, the transient regime so far was not developed. The need for simulations in the transient regime comes from the desire to handle large-signal response. The following topics consists of a break down of sub tasks that will be addressed.

.

2.1 The electromagnetic (EM) drift-diffusion (DD) solver in the time domain.

The MAGWEL software is build as a reusable, strongly object-oriented C++-code. The front-end needs only minor modification to set up the time domain control. The meshing algorithms can be fully reused. With these advantages in mind, it make sense to exploit these advantages. In particular, we can not only reuse the front-end but also the equation assembling can be done by reusing the algorithms for constructing the various terms.

2.2 EM-DD equations

Note: In this section, we will present our equations as $lhs = rhs$, for didactic reason. In a later stage we will collect our results as $lhs = 0$, for computational reasons.

2.2.1 Use of potentials

Our starting point will be the equations of Maxwell:

$$\text{Gauss' law:} \quad \nabla \cdot \mathbf{D} = \rho \tag{1}$$

$$\text{Absence of magnetic monopoles:} \quad \nabla \cdot \mathbf{B} = 0 \tag{2}$$

$$\text{Maxwell-Faraday:} \quad \nabla \times \mathbf{E} = -\frac{\partial \mathbf{B}}{\partial t} \tag{3}$$

$$\text{Maxwell-Ampère:} \quad \nabla \times \mathbf{H} = \mathbf{J} + \frac{\partial \mathbf{D}}{\partial t} \tag{4}$$

where $\mathbf{D}$, $\mathbf{E}$, $\mathbf{B}$, $\mathbf{H}$, $\mathbf{J}$ en ρ are the electric induction, the electric field, magnetic induction and magnetic field, current density and charge density.

The following constitutive laws are used:

$$\mathbf{B} = \mu \mathbf{H}, \qquad \mathbf{D} = \varepsilon \mathbf{E} \tag{5}$$

The charge density ρ and current density $\mathbf{J} = 0$ in insulating materials and charge density ρ consists of a fixed background charge. In conductive domains we rely on the current continuity:

$$\nabla \cdot \mathbf{J} + \frac{\partial \rho}{\partial t} = 0 \tag{6}$$

If these conductive domains are metallic, then we apply Ohm's law for the connection between electric field intensity and current density. It should be noted that this is not the most general

expression and for Hall devices a magnetic field dependence must also be included. However, here we limit ourselves to situations where the magnetic fields are sufficiently weak in order to ignore Hall currents:

$$\mathbf{J} = \sigma \mathbf{E} \tag{7}$$

It should also be noted that the charge density and current densities are determined by the physical character of the materials under study. For example leakage currents can flow in insulating layers and the current-field relation is highly non-linear since tunneling mechanisms play an important role. Semiconductors also have more general current-field relations as given above and these will be discussed later.

We introduce the scalar potential V en the magnetic vector potential $\mathbf{A}$ that satisfy

$$\mathbf{B} = \nabla \times \mathbf{A} \tag{8}$$

$$\mathbf{E} = -\nabla V - \frac{\partial \mathbf{A}}{\partial t} \tag{9}$$

then the Maxwell equation become in these variables;

- *for insulators:*

$$-\nabla \cdot \left[\varepsilon \left(\nabla V + \frac{\partial \mathbf{A}}{\partial t} \right) \right] = 0 \tag{10}$$

$$\nabla \times \frac{1}{\mu} (\nabla \times \mathbf{A}) = -\varepsilon \frac{\partial}{\partial t} \left(\nabla V + \frac{\partial \mathbf{A}}{\partial t} \right) \tag{11}$$

- *for conductors:*

$$-\nabla \cdot \sigma \left(\nabla V + \frac{\partial \mathbf{A}}{\partial t} \right) = \frac{\partial}{\partial t} \left(\nabla \cdot \varepsilon \left(\nabla V + \frac{\partial \mathbf{A}}{\partial t} \right) \right) \tag{12}$$

$$\nabla \times \frac{1}{\mu} (\nabla \times \mathbf{A}) = -\sigma \left(\nabla V + \frac{\partial \mathbf{A}}{\partial t} \right) - \varepsilon \frac{\partial}{\partial t} \left(\nabla V + \frac{\partial \mathbf{A}}{\partial t} \right) \tag{13}$$

For the description in the Fourier domain we replace each differentiation w.r.t. time by a factor $j\omega$, with j the imaginary unit and $\omega = 2\pi f$ the angular velocity and f is the operational frequency.

These differential equations are with the MAGWEL software discretized in 3D-space using the finite-volume method (FVM) and finite-surface method (FSM). Whereas the FVM is based on averaging variables over cells to obtain discrete variables the FSM averages method obtains discrete variables by averaging over surfaces. These averaging procedures apply Gauss' law (FVM) and Stokes' law (FSM). The success of the method is based on respecting the geometrical origin of the various variables that are encountered in the mathematical set up.

For the description in the time domain we can reuse the spatial discretization methods. However, we will end up with a second-order differentiation in time. Part of the research in this WP will be to give a procedure for a correct treatment of these terms. Physically, the second order time-derivative terms illustrate the wave delay that is found in the Maxwell equations. A popular argument for handling these terms is based on considering the scales of application. In particular, if we are operating in the below 100 GHz range, the wave length is 3 mm=3000 microns. Assuming that typical lengths inside the chip is below this figure, it is argued that these 2nd order time derivatives could be ignored. Thus a 'crude' method just ignores the second order time differential on $\mathbf{A}$. As a consequence we arrive at some form of a quasi-static

approximation and one is not accounting for the delay induced by wave propagation. Another way of looking at this approximation is to assume that speed of light is infinity. In the PEEC method this approximation is exploited *PEEC* (Partial Element Equivalent Circuit Method).

Dropping terms out of equations should be done with care. Although a term may seem irrelevant on an instantaneous view, it must be considered also from the view how it participates in keeping the global behavior physically correct. For instance, spontaneous creation of charge is prohibited and dropping one term might induce the need to drop corresponding terms for physical consistency. In order to explore these pitfalls, we propose another representation.

The second approach introduces a new variable the *pseudo-canonical momentum* $\Pi = \partial \mathbf{A}/\partial t$. We may rewrite the system of equations as (e.g. for a conductor):

$$
\begin{aligned}
-\nabla \cdot \sigma \left(\nabla V + \mathbf{\Pi} \right) &= \nabla \cdot \varepsilon \left(\nabla \frac{\partial V}{\partial t} + \frac{\partial \mathbf{\Pi}}{\partial t} \right) && (14) \\
\nabla \times \left(\frac{1}{\mu} \nabla \times \mathbf{A} \right) &= -\sigma \left(\nabla V + \frac{\partial \mathbf{A}}{\partial t} \right) - \varepsilon \left(\nabla \frac{\partial V}{\partial t} + \frac{\partial \mathbf{\Pi}}{\partial t} \right) && (15) \\
\mathbf{\Pi} &= \frac{\partial \mathbf{A}}{\partial t} && (16)
\end{aligned}
$$

We refer to the variable $\mathbf{\Pi}$ as a *pseudo*-canonical momentum, because when deriving the field equations from an Lagrange action, the electric field $-\mathbf{E}$ is found as the canonical conjugate to $\mathbf{A}$. The difference between the pseudo-canonical momentum and the canonical momentum is

$$\mathbf{\Pi} = -\mathbf{E} - \nabla V \tag{17}$$

2.2.2 Gauge conditions

The Equations (12-13) do not uniquely determine $\mathbf{A}$ and V. A solution can be $\mathbf{A}$, V can be adapted with a arbitrary scalar field χ

$$
\begin{aligned}
\mathbf{A}^{'} &= \mathbf{A} + \nabla \chi \\
V^{'} &= V - \frac{\partial \chi}{\partial t}
\end{aligned}
$$

which results into an equally valid solution of (12-13). After discretization the coefficient-matrix is singular. Additional equations must be added to elevate this singularity. These extra equations are the gauge conditions.

For the Coulomb gauge the following constraint is applied:

$$\nabla \cdot \mathbf{A} = \mathbf{0} \tag{18}$$

The Lorentz gauge is inspired by dealing with the term $\epsilon \nabla \left(\frac{\partial V}{\partial t} \right)$ in the Ampere-Maxwell equation:

$$\frac{1}{\mu} \nabla \left(\nabla \cdot \mathbf{A} \right) + \epsilon \nabla \left(\frac{\partial V}{\partial t} \right) = 0 \tag{19}$$

Usually we encounter the Lorenz gauge condition as

$$\nabla \cdot \mathbf{A} + \mu \epsilon \frac{\partial V}{\partial t} = 0 \tag{20}$$

However, we prefer to keep it in the form (19) because we need it in this way and moreover the form (20) is only equivalent to (19) for μ and ϵ constant. The pre-factor $1/\mu$ is a choice which is convenient in our field of application (EDA). We are dealing mostly with materials that are not ferromagnetic. Then $\mu_r = 1$, which allows an efficient evaluation of the Maxwell-Ampere equation.

Above argument is somewhat 'naive'. Actually, we do skip two terms in the Ampere-Maxwell equation by first adding and subtracting $1/\mu\nabla\left(\nabla\cdot\mathbf{A}\right)$ and use one to regularize the double curl operator.

For later use, we write the Lorentz gauge condition as

$$\epsilon\nabla\left(\frac{\partial V}{\partial t}\right) = -\frac{1}{\mu}\nabla\left(\nabla\cdot\mathbf{A}\right) \tag{21}$$

The Maxwell-Ampere equation can be written as

$$\epsilon\frac{\partial\mathbf{\Pi}}{\partial t} = -\nabla\times\left(\frac{1}{\mu}\nabla\times\mathbf{A}\right) + \frac{1}{\mu}\nabla\left(\nabla\cdot\mathbf{A}\right) - \sigma\nabla V - \sigma\mathbf{\Pi} \tag{22}$$

Furthermore, remember that

$$\frac{\partial\mathbf{A}}{\partial t} = \mathbf{\Pi} \tag{23}$$

then we arrive at the following condensed notation for the transient description

$$\varepsilon\frac{\partial}{\partial t}\begin{bmatrix} V \\ \mathbf{A} \\ \mathbf{\Pi} \end{bmatrix} = \mathcal{K}*\begin{bmatrix} V \\ \mathbf{A} \\ \mathbf{\Pi} \end{bmatrix} + \mathcal{B}*\begin{bmatrix} V_{dbc} \\ \mathbf{A}_{dbc} \\ \mathbf{\Pi}_{dbc} \end{bmatrix} \tag{24}$$

where $\mathcal{K}$ is a 3x3 matrix that can be generated in the MAGWEL solver, and $\mathcal{B}$ is an operator acting on the boundary-condition prescribed values. The $V_{dbc}, \mathbf{A}_{dbc}$ and $\mathbf{\Pi}_{dbc}$ are given values Dirichlet boundaries. In Section 4, examples are given.

The $\mathcal{K}$ matrix represents the following operators:

$$\mathcal{K} = \begin{bmatrix} 0 & -\frac{1}{\mu}\nabla\cdot & 0 \\ 0 & 0 & \epsilon \\ -\sigma\nabla & -\nabla\times\left[\frac{1}{\mu}\nabla\times\ \ \right] + \frac{1}{\mu}\nabla\left[\nabla\cdot\ \ \right] & -\sigma \end{bmatrix} \tag{25}$$

It is important to realize that a *transient* simulator solves the temporal evolution in terms of:

- The *gauge condition* for computing the changes in time of V
- The *definition* of the pseudo-canonical momentum $\mathbf{\Pi}$ for computing the changes in time of $\mathbf{A}$
- The *Maxwell-Ampere equation* for computing the changes in time of $\mathbf{\Pi}$.
- Gauss law does *not* play a role for determining the time-evolution, but informs us that we can not start from an arbitrary $(V, \mathbf{A}, \mathbf{\Pi})$ - configuration, but one that satisfies Gauss' law.

The last item is illustrated in Fig. 1. In the $(V, \mathbf{A}, \mathbf{\Pi})$ - configuration space there is a hyper surface compliant with Gauss' law. An initial point should be located at this hyper surface. Next the time-evolution operator $\mathcal{K}$ should guarantee that the flow remains on this hyper surface.

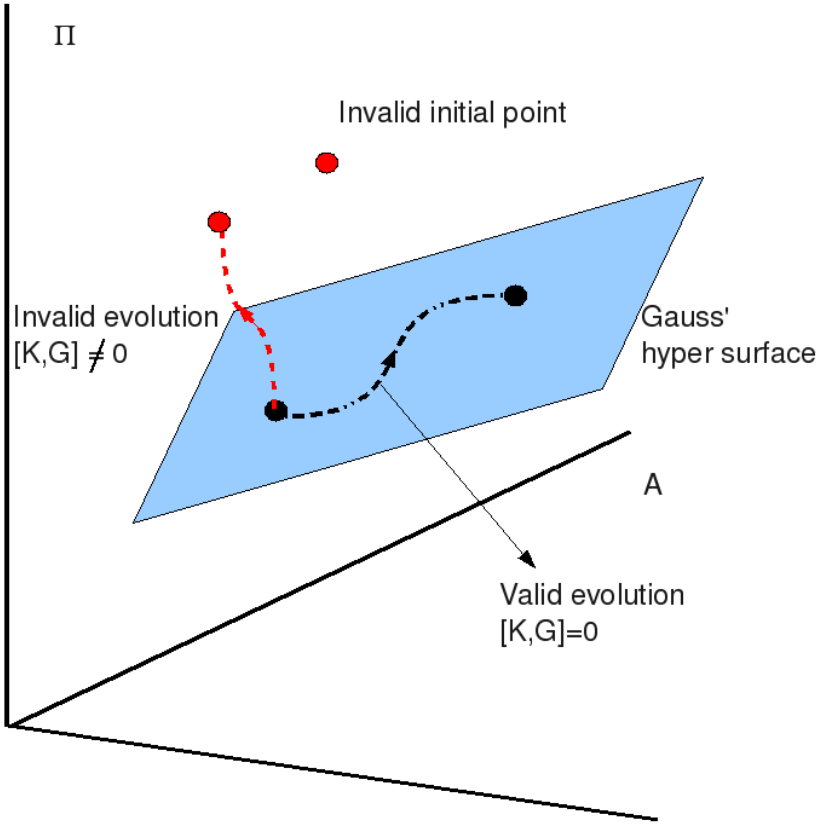

Figure 1: Illustration of the use of Gauss' law.

2.2.3 Semiconductor treatment

For the simulation of semiconductor regions we use the current-continuity equations

$$\nabla \cdot \mathbf{J}_{\mathrm{n}} - q\frac{\partial n}{\partial t} = U(n,p), \tag{26}$$

$$\nabla \cdot \mathbf{J}_{\mathrm{p}} + q\frac{\partial p}{\partial t} = -U(n,p). \tag{27}$$

Here, n and p are the electron and hole concentrations and $U(n,p)$ represent the generation/recombination mechanisms. The drift-diffusion model provides us with explicit relations between the electron and hole current densities and the electric field intensity as well as the carrier concentration

$$\mathbf{J}_{\mathrm{n}} = q\mu_{\mathrm{n}} n\mathbf{E} + qkT\mu_{\mathrm{n}}\nabla n, \tag{28}$$

$$\mathbf{J}_{\mathrm{p}} = q\mu_{\mathrm{p}} p\mathbf{E} - qkT\mu_{\mathrm{p}}\nabla p. \tag{29}$$

The charge density ρ is

$$\rho = q(p - n + N_{\mathrm{D}} - N_{\mathrm{A}}) \tag{30}$$

The carrier concentrations are modeled using the Boltzmann distribution, i.e. the amount of carriers with a given amount of energy is proportional to the exponential of the $-E/kT$. Introducing the Fermi potentials ϕ_n and ϕ_p the following relation holds:

$$n = n_i\, \mathrm{e}^{\frac{q}{kT}(V-\phi_n)}, \qquad p = n_i\, \mathrm{e}^{\frac{q}{kT}(\phi_p - V)},$$

and n_i is the intrinsic carrier concentration.

We can add the following set of equations for the description of semiconductors (10-13)

$$-\nabla\cdot\varepsilon\left(\nabla V + \frac{\partial \mathbf{A}}{\partial t}\right) = qn_i\, \mathrm{e}^{\frac{q}{kT}(\phi_p - V)} - qn_i\, \mathrm{e}^{\frac{q}{kT}(V-\phi_n)} + N_{\mathrm{D}} - N_{\mathrm{A}} \tag{31}$$

$$\begin{aligned}\nabla \times \frac{1}{\mu}(\nabla \times \mathbf{A}) = {} & q\mu_p n_i\, \mathrm{e}^{\frac{q}{kT}(\phi_p - V)}\left(\nabla V + \frac{\partial \mathbf{A}}{\partial t}\right) - qkT\mu_p \nabla n_i e^{\frac{q}{kT}(\phi_p - V)} \\ & + q\mu_n n_i\, \mathrm{e}^{\frac{q}{kT}(V-\phi_n)}\left(\nabla V + \frac{\partial \mathbf{A}}{\partial t}\right) + qkT\mu_n \nabla n_i e^{\frac{q}{kT}(V-\phi_n)} \\ & - \varepsilon\frac{\partial}{\partial t}\left(\nabla V + \frac{\partial \mathbf{A}}{\partial t}\right)\end{aligned} \tag{32}$$

$$\begin{aligned}\nabla\cdot\left(q\mu_p\, n_i \mathrm{e}^{\frac{q}{kT}(\phi_p - V)}\left(\nabla V + \frac{\partial \mathbf{A}}{\partial t}\right) - qkT\mu_p \nabla e^{\frac{q}{kT}(\phi_p - V)}\right) = {} & -U(n,p) \\ & - qn_i\frac{\partial}{\partial t}\left(\mathrm{e}^{\frac{q}{kT}(\phi_p - V)}\right)\end{aligned} \tag{33}$$

$$\begin{aligned}\nabla\cdot\left(q\mu_n\, n_i \mathrm{e}^{\frac{q}{kT}(V-\phi_n)}\left(\nabla V + \frac{\partial \mathbf{A}}{\partial t}\right) + qkT\mu_n \nabla e^{\frac{q}{kT}(V-\phi_n)}\right) = {} & U(n,p) \\ & + qn_i\frac{\partial}{\partial t}\left(e^{\frac{q}{kT}(V-\phi_n)}\right)\end{aligned} \tag{34}$$

We have presented here all expressions explicitly in terms of the potentials in order to illustrate the non-linear character of the equation system.

The set of unknowns $(V, \mathbf{A}, \mathbf{\Pi})$ needs to be extended with the Fermi levels ϕ_p and ϕ_n or alternatively with p and n. In this case we can add the following set of equations for the description of semiconductors (10-13)

$$
\begin{aligned}
-\nabla \cdot \varepsilon \left(\nabla V + \frac{\partial \mathbf{A}}{\partial t} \right) &= q(p-n) + N_{\mathrm{D}} - N_{\mathrm{A}} && (35)\\
\nabla \times \frac{1}{\mu} (\nabla \times \mathbf{A}) &= \underbrace{-q\mu_p p \left(\nabla V + \frac{\partial \mathbf{A}}{\partial t} \right) - qkT\mu_p \nabla p}_{:=\mathbf{J}_p} && (36)\\
&\quad \underbrace{-q\mu_n n \left(\nabla V + \frac{\partial \mathbf{A}}{\partial t} \right) + qkT\mu_n \nabla n}_{:=\mathbf{J}_n} && (37)\\
&\quad -\varepsilon \frac{\partial}{\partial t} \left(\nabla V + \frac{\partial \mathbf{A}}{\partial t} \right) && (38)\\
\nabla \cdot \left(q\mu_p p \left(\nabla V + \frac{\partial \mathbf{A}}{\partial t} \right) - qkT\mu_p \nabla p \right) &= -U(n,p) - q\frac{\partial p}{\partial t} && (39)\\
\nabla \cdot \left(q\mu_n n \left(\nabla V + \frac{\partial \mathbf{A}}{\partial t} \right) + qkT\mu_n \nabla n \right) &= U(n,p) + q\frac{\partial n}{\partial t} && (40)
\end{aligned}
$$

In the frequency domain we have linearized the equation at some operation point

$$X_{op} = (\mathbf{E}_0, p_0, n_0) \tag{41}$$

$$
\begin{aligned}
\mathbf{J}_{\mathrm{n}} &= q\mu_{\mathrm{n}} n_0 \mathbf{E} + q\mu_{\mathrm{n}} n \mathbf{E}_0 + qkT\mu_{\mathrm{n}} \nabla n && (42)\\
\mathbf{J}_{\mathrm{p}} &= q\mu_{\mathrm{p}} p_0 \mathbf{E} + q\mu_{\mathrm{p}} p \mathbf{E}_0 - qkT\mu_{\mathrm{p}} \nabla p, && (43)
\end{aligned}
$$

where the operation point is determined by a solution of the static bias conditions $(\mathbf{E}_0, p_0, n_0)$. In the time domain, we are interested in a direct integration in time to explore the solution. Linearization methods will have only restricted value.

3 Implementation of numerical methods for solving the equations

3.1 Introduction

The discretization procedure will be separated into two parts. First we will described the handling of the fields on the discrete spatial grid. After the spatial discretization, we have transform our problem definition from having a finite set of fields $\psi_n(\mathbf{x}, t)$ to a lattice of variables $\psi_{n,k}(t)$, where n is an index to the field under consideration e.g. $V, \mathbf{A}, \phi_p, \phi_n$ and k labels a grid object, i.e. a node or a link. So far each variable is still a continuous function of time. In the second part, we will discuss how the transient problem will be numerically addressed.

3.2 Spatial discretization

In order to solve the continuous partial differential equations a transition must be made to a discretization grid. How this is done in general is well-known in the literature. Here, we will emphasize the main ingredients as well as the subtle details that come with our specific set of equations under consideration.

A convenient mental picture is to address the discretization in three steps: First we replace the continuous 'universe' by a lattice of discrete points. Next we replace the continuous differential operators by local coupling between neighboring lattice points, and thirdly, we cut out of the 'entire universe' a finite portion and give conditions (usually idealized ones) how the rest of universe interferes with the portion under consideration. We refer to this finite portion as the simulation domain, Ω which has an enclosing surface $\partial\Omega$. In a nutshell this is what discretization is about. Already right at the start we encounter a subtle detail. Cutting out a piece out of large geometrical entity and remembering that our starting equations have a local character, it would mean that the impact of the external domain would take place only via the surface of the simulation domain. In other words boundary conditions are expected on the surface $\partial\Omega$. Although this makes sense from a mathematical perspective, it has been shown beneficial to allow for 'internal' boundary conditions also. Since the external part is not part of our computation problem ("by definition") all the lattice variables are corresponding to this part have no representation in the computer memory. There presence is absorbed in a series of restrictions for the lattice variables of the internal, i.e. those variables that have a chunk of memory allocated. Within this view, one may consider boundary conditions as a set of limitations to construct a solvable problem only the word 'boundary' should not be taken too literally.

3.2.1 Discretization of Gauss' law

As an illustration of the discretization method, we will here discretize Gauss' law [2]. The starting equation is

$$-\nabla\left[\epsilon\left(\nabla V + \frac{\partial \mathbf{A}}{\partial t}\right)\right] - \rho = 0 \tag{44}$$

On a discretization grid we consider the Voronoi cells around each node, say i, of the grid and

[2] It should be emphasized that the purpose of this section is to show typical discretization steps. Remember that the role of Gauss' law is to provide constraints on the initial values and that the time evolution should be compliant with it.

take take the volume integral of equation (44). Applying Gauss' law we find that

$$\int_{\partial(\Delta v)} \mathbf{dS} \cdot (-\epsilon) \left(\nabla V + \frac{\partial \mathbf{A}}{\partial t} \right) - Q(\Delta v) = 0 \tag{45}$$

Using the geometrical information of the Voronoi cells this amounts to adding all contribution from each link that ends or begins in node i

$$\sum_j \epsilon \left[\frac{S_{ij}}{h_{ij}} (V_i - V_j) - \sigma_{ij} \frac{\mathrm{d}A_{ij}}{\mathrm{d}t} S_{ij} \right] - Q_i = 0. \tag{46}$$

In this expression, the sum j is over all neighboring nodes. S_{ij} is the perpendicular area for the link connecting node i and node j. The variable h_{ij} is the length of the link ij. Furthermore, A_{ij} is the projection of the vector potential on link (ij) and is also a degree of freedom. The variable $\sigma_{ij} = \pm 1$. It represents the relative orientation of the vector potential with respect to the grid orientation.

3.2.2 Boundary conditions for Gauss' discretized law

We are now in the position to consider the boundary conditions for above set of equations. Let $\mathcal{N}_\infty$ be the collection of all lattice nodes and links for the 'universe', let $\mathcal{N}_{sim}$ be the collection of all lattice nodes and link that participate in the simulation problem. How can we get rid off $\mathcal{N}_\infty - \mathcal{N}_{sim}$? A simple idea is that there are parts of the surface of the simulation domain where the interaction is not present. This means that the perpendicular displacement at $\partial\Omega$ is zero, i.e $\mathbf{D}.\mathbf{n} = 0$. As a consequence, we can assemble (46) just as if the the rest of the universe does not exists. The assembling is illustrated in the introduction. This approach is known as putting Neumann boundary conditions.

Another elimination procedure is to assume that the impact of the rest of the universe is screened off by prescribed values at (other) segments of $\partial\Omega$. Voltage sources are a physical realization. These are the Dirichlet's boundary conditions.

We can now consider equation (46) in more detail. Actually as it stands it reads as follows:

$$\sum_j \epsilon \left[\frac{S_{ij}}{h_{ij}} (V_i - V_j) - \sigma_{ij} \frac{\mathrm{d}A_{ij}}{\mathrm{d}t} S_{ij} \right] - Q_i = 0 \qquad\qquad i \subset \mathcal{N}_\infty \tag{47}$$

This is now further specified as follows: The set $\mathcal{N}_{sim}$ consists of two groups. The first set contains the true degrees of freedom. We refer to this set as $\mathcal{N}_{sim}^{dof}$. The second set contains the Dirichlet boundary condition set, denoted as $\mathcal{N}_{sim}^{dbc}$. Let us also introduce a notational convenience: time derivatives will be denoted with a dot.

$$\sum_j \epsilon \left[\frac{S_{ij}}{h_{ij}} (V_i - V_j) - \sigma_{ij} \dot{A}_{ij} S_{ij} \right] - Q_i = 0 \qquad\qquad i \subset \mathcal{N}_{sim}^{dof} \tag{48}$$

Next we can consider the sum at the left-hand side. For each degree-of-freedom, we can separate the sum into two sets also. The first set contains the coupling to other degrees of freedom ('internal' nodes) and the second set contains the coupling to the Dirichlet boundary

nodes. Thus we obtain

$$\sum_{j\subset\mathcal{N}_{sim}^{dof}} \epsilon\left[\frac{S_{ij}}{h_{ij}}\left(V_i-V_j\right)-\sigma_{ij}\dot{A}_{ij}S_{ij}\right]+\sum_{j\subset\mathcal{N}_{sim}^{dbc}} \epsilon\left[\frac{S_{ij}}{h_{ij}}\left(V_i-V_j\right)-\sigma_{ij}\dot{A}_{ij}S_{ij}\right]-Q_i=0$$
$$i\subset\mathcal{N}_{sim}^{dof} \qquad (49)$$

Finally, the second sum can be split as shown below:

$$\sum_{j\subset\mathcal{N}_{sim}^{dof}} \epsilon\left[\frac{S_{ij}}{h_{ij}}\left(V_i-V_j\right)-\sigma_{ij}\dot{A}_{ij}S_{ij}\right]+V_i\sum_{j\subset\mathcal{N}_{sim}^{dbc}}\epsilon\frac{S_{ij}}{h_{ij}}$$
$$-\sum_{j\subset\mathcal{N}_{sim}^{dbc}}\sigma_{ij}\dot{A}_{ij}S_{ij}-Q_i \;=\; \sum_{j\subset\mathcal{N}_{sim}^{dbc}}\epsilon\frac{S_{ij}}{h_{ij}}V_j, \qquad i\subset\mathcal{N}_{sim}^{dof}$$

Recognizing all V_i as degrees of freedom and all V_j as prescribed values we see that the discretized system finally take the form:

$$\mathbf{A}*\mathbf{x}=\mathbf{b} \qquad (50)$$

Here, we assumed that ρ and therefore Q_i is independent of the voltages. For semiconductors being present this is not true, and we end up with a system that is non-linear in the voltages. Then Newton-Raphson schemes are needed to solve the full system.

We have not mentioned yet the detailed discretization for the projected vector potentials however, as for as the discussion for the Gauss' law is concerned, all A_{ij} are degrees of freedom. This is because the the links on $\partial\Omega$ have a simple Dirichlet-type boundary condition, $A_{ij}=0 \quad (ij)\subset\partial\Omega$. In fact, this matrix consists of two parts in this example. To be more precise, it takes the form

$$\left(\mathbf{A}_0+\mathbf{A}_1\frac{\mathrm{d}}{\mathrm{d}t}\right)*\mathbf{x}=\mathbf{b} \qquad (51)$$

where $\mathbf{A}_1$ acts on the link degrees of freedom.

3.3 Discretization of current-continuity equations

In order to get a better insight in the EM equations and how their transient versions are designed, we will present here a detailed derivation of the current-continuity equation in metallic regions.

$$\nabla\cdot\mathbf{J}+\frac{\partial\rho}{\partial t}=0 \qquad (52)$$

In here,

$$\rho=\nabla\cdot\mathbf{D} \qquad (53)$$

Furthermore,

$$\begin{aligned}\mathbf{E} &= -\nabla V-\frac{\mathbf{A}}{\partial t}\\ \mathbf{\Pi} &= \frac{\partial\mathbf{A}}{\partial t}\\ \mathbf{E} &= -\nabla V-\mathbf{\Pi}\end{aligned} \qquad (54)$$

For each link the discretized version of $\mathbf{E}$ is

$$E_{ij} = -\frac{1}{h_{ij}} \left(V_j - V_i + s_{ij}\Pi_{ij}\ h_{ij}\right) \tag{55}$$

In here, $s_{ij} = \pm 1$ is depending on the link orientation. Let σ_{ij} be the conductance associated the the link $< ij >$. Then the discretized current-continuity equation takes the following form :

$$\sum_j \frac{d_{ij}}{h_{ij}} \varepsilon \frac{\partial}{\partial t} \left(V_j - V_i + s_{ij}\Pi_{ij}\ h_{ij}\right) + \sum_j \frac{d_{ij}}{h_{ij}} \sigma_{ij} \left(V_j - V_i + s_{ij}\Pi_{ij}\ h_{ij}\right) = 0 \tag{56}$$

From this equation we can read off the content of the matrix $\tilde{A}$. Furthermore, the current - continuity equation for metals has the property that the function $\tilde{d}$ is trivial.

Remember that we could construct the EM system in two ways: 1) we exploit the Gauss' law and after a complete discretization , the gauge condition is a side-product; 2) we discretize Gauss' law and the gauge condition is side product. Let us purchase the second option. For insulating regions (interior nodes!) we obtain the discretized Gauss' law in the following form

$$\varepsilon \frac{d_{ij}}{h_{ij}} \left(V_i - V_j - s_{ij}\Pi_{ij}\ h_{ij}\right) = 0 \tag{57}$$

Note that there is no term containing a time differentiation. The corresponding content of the $\tilde{A}$ matrix is zero. Physically, this equation is a *constraint* , as was extensively discussed in D3.2.

Next let us consider an *interior* semiconductor node. First of all Gauss' law gets modified by a charge contribution.

$$\varepsilon \frac{d_{ij}}{h_{ij}} \left(V_i - V_j - s_{ij}\Pi_{ij}\ h_{ij}\right) - p_i(\phi_i^p, V_i)\ \Delta w_i + n_i(\phi_i^n, V_i)\ \Delta w_i + N_D\ \Delta w_i\ = 0 \tag{58}$$

in which w_i is nodal volume. All time dependence is *implicit* . Therefore, this equation still is a constraint. The hole and electron concentrations are given by

$$\begin{aligned} p &= n_0 \exp\left(\phi^p - V\right) \\ n &= n_0 \exp\left(V - \phi^n\right) \end{aligned} \tag{59}$$

where n_0 is the intrinsic concentration.

For the intrinsic semiconductor nodes we must also solve the current-continuity equations

$$\begin{aligned} \frac{\partial}{\partial t} p + \nabla \cdot \mathbf{J}_p + qR = 0 \\ \frac{\partial}{\partial t} n - \nabla \cdot \mathbf{J}_n + qR = 0 \end{aligned} \tag{60}$$

For the discretized hole currents we obtain using the Scharfetter-Gummel discretization scheme

$$J_{ij}^p = \mu_p \frac{d_{ij}}{h_{ij}} \left(p_i B[X_{ij}] - p_j B[-X_{ij}]\right) \tag{61}$$

where

$$X_{ij} = V_j - V_i + s_{ij} h_{ij} \Pi_{ij} \tag{62}$$

and $B(x) = x/(e^x - 1)$ is the Bernoulli function. Note that the function $R = R(p, n)$.

the equation for the electron current is :

$$J^n_{ij} = -\mu_n \frac{d_{ij}}{h_{ij}} \left(n_i B[-X_{ij}] - n_j B[X_{ij}] \right) \tag{63}$$

The hole equation for node i is

$$\Delta w_i \frac{\partial}{\partial t} p_i + \sum_j \mu_p \frac{d_{ij}}{h_{ij}} \left(p_i B[X_{ij}] - p_j B[-X_{ij}] \right) + R(p_i, n_i) \Delta w_i = 0 \tag{64}$$

In here, w_i is the nodal volume. In a slightly modified version it reads :

$$\Delta w_i \; n_0 \frac{\partial}{\partial t} \mathrm{e}^{(\phi^p_i - V_i)} + \sum_j \mu_p \frac{d_{ij}}{h_{ij}} \left(p_i B[X_{ij}] - p_j B[-X_{ij}] \right) + R(p_i, n_i) \Delta w_i = 0 \tag{65}$$

Thus the function $\tilde{d}$ is simply the exponential of the difference of the elementary variables $\phi^p - V$.

For the electrons we have :

$$\Delta w_i \; n_0 \frac{\partial}{\partial t} \mathrm{e}^{(V_i - \phi^n_i)} + \sum_j \mu_n \frac{d_{ij}}{h_{ij}} \left(n_i B[-X_{ij}] - n_j B[X_{ij}] \right) + R(p_i, n_i) \Delta w_i = 0 \tag{66}$$

The function $\tilde{d} = \mathrm{e}^{(V - \phi^n)}$.

Besides the subtleties of the discretization that need to be considered at material interfaces, above scheme gives a rather complete overview of the time evolution for the the variables V, ϕ^p, ϕ^n.

3.4 Discretization of the Maxwell-Ampere system

Just as for nodal variables, the entities associated to other geometrical objects, such as links or surfaces, we must first limit ourselves to a finite subset of links. Whereas Equation (22) is written down for the complete 'universe', a domain restriction is required. Suppose, we have a finite domain Ω selected. Furthermore, a grid is built using the nodes that were identified in the foregoing section. Next, we focus on all the links that connect these nodes. Again, some links will be found on the surface of Ω, to be precise, $(ij) \in \partial\Omega$. The construction of the equations of motion (and/or constrain equations) requires special care, because the finite-integration methods around such links we bring us outside Ω and that falls outside the region for which we compute information. We will first consider the situation when (ij) is an internal link, i.e. the link is not at the surface of the simulation domain.

Let us start with the Maxwell-Ampere equation and consider for each link its dual surface. We will take the integral of this equation over the dual surface. Furthermore, we multiply the results with the length L of the link and obtain

$$\begin{aligned} \epsilon L \frac{\partial}{\partial t} \int_{\Delta S} \mathrm{d}\mathbf{S} \cdot \mathbf{\Pi} \;\; + \;\; L \int_{\Delta S} \mathrm{d}\mathbf{S} \cdot \nabla \times \left(\frac{1}{\mu} \nabla \times \mathbf{A} \right) - L \int_{\Delta S} \mathrm{d}\mathbf{S} \cdot \frac{1}{\mu} \nabla \left(\nabla \cdot \mathbf{A} \right) \\ + L \int_{\Delta S} \mathrm{d}\mathbf{S} \cdot \sigma \nabla V \;\; + \;\; L \int_{\Delta S} \mathrm{d}\mathbf{S} \cdot \sigma \mathbf{\Pi} \;\; = \;\; 0 \end{aligned} \tag{67}$$

Here, we put the equation in the appearance $lhs = 0$.

The discretization of each term will now be discussed. Starting at the left-hand side, we define a link variable Π_{ij} for the link going from node i to node j. The surface integral is approximated by taking $\mathbf{\Pi}$ constant over the dual area. Thus

$$\epsilon L \, \frac{\partial}{\partial t} \int_{\Delta S} \mathrm{d}\mathbf{S} \cdot \mathbf{\Pi} \simeq \epsilon L \, \Delta S_{ij} \, \frac{d\Pi_{ij}}{dt} \tag{68}$$

We can assign to each link a volume being $\Delta v_{ij} = L \, \Delta S_{ij}$. The second term on the right-hand side is dealt with using Stokes theorem twice in order to evaluate the circulations.

$$L \int_{\Delta S} \mathrm{d}\mathbf{S} \cdot \nabla \times \left(\frac{1}{\mu} \nabla \times \mathbf{A} \right) = L \oint_{\partial(\Delta S)} \mathrm{d}\mathbf{l} \cdot \left(\frac{1}{\mu} \nabla \times \mathbf{A} \right) \tag{69}$$

The circumference $\partial(\Delta S)$ consists of N segments. Each segment corresponds to a dual link that pierces through a *primary* surface. Therefore, we may approximate the right-hand side of (69) as

$$L \oint_{\partial(\Delta S)} \mathrm{d}\mathbf{l} \cdot \left(\frac{1}{\mu} \nabla \times \mathbf{A} \right) = L \sum_{k=1}^{N} \Delta l_k \, \frac{1}{\mu_k} \, \left(\nabla \times \mathbf{A} \right)_k \tag{70}$$

where the sum goes over all primary surfaces that were identified above as belonging to the circulation around the starting link. Note that we also attached an index on μ. This will guarantee that the correct value is taken depending in which material the segment Δl_k is located.

Next we must obtain an appropriate expression for $\left(\nabla \times \mathbf{A} \right)_k$. For that purpose, we consider the primary surfaces. In particular, an approximation for this expression is found by using

$$\left(\nabla \times \mathbf{A} \right)_k \simeq \frac{1}{\Delta S_k} \int_{\Delta S_k} \mathrm{d}\mathbf{S} \cdot \nabla \times \mathbf{A} = \frac{1}{\Delta S_k} \oint_{\partial(\Delta S_k)} \mathrm{d}\mathbf{l} \cdot \mathbf{A} \tag{71}$$

The last contour integral is evidently replaced by the collection of primary links variables around the primary surface. As a consequence, the second term at the right-hand side of (67) becomes

$$L \sum_{k=1}^{N} \Delta l_k \, \frac{1}{\mu_k} \, \frac{1}{\Delta S_k} \left(\sum_{l=1}^{N'} \Delta l_{<kl>} A_{<kl>} \right) \tag{72}$$

where we distinguished the link labeling from node labeling (ij) to surface labeling $< kl >$.

So finally, we obtain

$$L \int_{\Delta S} \mathrm{d}\mathbf{S} \cdot \nabla \times \left(\frac{1}{\mu} \nabla \times \mathbf{A} \right) = L \sum_{k=1}^{N} \Delta l_k \, \frac{\alpha}{\mu_k} \, \frac{1}{\Delta S_k} \left(\sum_{l=1}^{N'} \Delta l_{<kl>} A_{<kl>} \right) \tag{73}$$

Next we consider the third term of (67). Now we use the fact that each link has a specific orientation from 'front' to 'back'.

$$-L \int_{\Delta S} \mathrm{d}\mathbf{S} \cdot \frac{1}{\mu} \nabla \left(\nabla \cdot \mathbf{A} \right) \simeq - \int_{\Delta S} \mathrm{d}\mathbf{S} \cdot \frac{1}{\mu} \left(\nabla \cdot \mathbf{A} \right)_{back} + \int_{\Delta S} \mathrm{d}\mathbf{S} \cdot \frac{1}{\mu} \left(\nabla \cdot \mathbf{A} \right)_{front} \tag{74}$$

The link orientation coding is illustrated in Fig. 2.

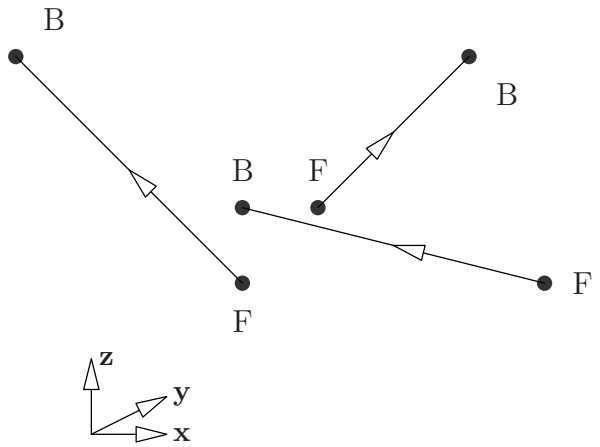

Figure 2: A collection of oriented links.

The two term in (74) are now discretized as

$$\begin{aligned}\int_{\Delta S} \mathrm{d}\mathbf{S} \cdot \frac{1}{\mu} (\nabla \cdot \mathbf{A}) &= \frac{\Delta S}{\mu \Delta v} \int_{\Delta v} \mathrm{d}v \nabla \cdot \mathbf{A} \\ &= \frac{\Delta S}{\mu \Delta v} \oint_{\partial(\Delta v)} \mathrm{d}\mathbf{S} \cdot \mathbf{A} \\ &= \frac{\Delta S}{\mu \Delta v} \sum_{j}^{n} \Delta S_{ij} A_{ij} \end{aligned} \tag{75}$$

where the sum is now from the front or back node to their corresponding neighbor nodes. The boundary conditions enter this analysis in a specific way. Suppose the front or back node is on the surface of the simulation domain. Then the closed surface integral around such a node will require a dual area contribution from a dual area outside the simulation domain. These surfaces are by definition not considered.

However, we can go back to the gauge condition and use

$$\int_{\Delta S} \mathrm{d}\mathbf{S} \cdot \frac{1}{\mu} (\nabla \cdot \mathbf{A}) = -\Delta S \, \epsilon \frac{\partial V}{\partial t}. \tag{76}$$

At first sight this looks weird: First we insert the gauge condition to get rid of the singular character of the curl-curl operation and now we 'undo' this for nodes at the surface. This is however fine because for Dirichlet boundary conditions for $\mathbf{A}$ there are no closed circulations around primary surfaces and there there is no uniqueness problem and therefore the operator is well defined.

The last two terms are rather straightforward: For the fourth term we consider ∇V constant over the dual surface. Thus we obtain

$$L \int_{\Delta S} \mathrm{d}\mathbf{S} \cdot \sigma \nabla V = (V_{back} - V_{front}) \left(\sum \Delta S_i \sigma_i \right). \tag{77}$$

The variation of σ is taken into account by looking at each volume contribution separately.

The fourth term can be dealt with in a similar manner.

$$L \int_{\Delta S} \mathrm{d}\mathbf{S} \cdot \sigma \mathbf{\Pi} = L \, \Pi_{ij} \, \left(\sum \Delta S_i \sigma_i \right). \tag{78}$$

Collecting all terms, we come to the following structure for the discretized Maxwell-Ampere equation :

- Assuming Dirichlet's boundary conditions for the vector potential on the simulation domain boundary, we are dealing only with link degrees of freedom (DOF) corresponding to link that are inside the simulation domain.
- Assuming Neumann's boundary conditions, the links at the surface of the simulation domain also generate degrees of freedom.
- Each DOF-generating link induces two variables: A and Π, where $A = \mathbf{A}\cdot\mathbf{n}$ and $\Pi = \mathbf{\Pi}\cdot\mathbf{n}$ where $\mathbf{n}$ is the intrinsic link orientation,
- The Maxwell-Ampere equation is a time-evolution equation for $\mathbf{\Pi}$
- The time-evolution equation depends on V, A and Π as is summarized below.

$$\hat{\epsilon}\frac{\mathrm{d}}{\mathrm{d}t}\mathbf{\Pi} + M * \mathbf{V} + N * \mathbf{A} + \hat{\sigma} * \mathbf{\Pi} = 0 \qquad \mathbf{V} = \begin{bmatrix} V_1 \\ \cdot \\ \cdot \\ V_n \end{bmatrix} \qquad \mathbf{A} = \begin{bmatrix} A_1 \\ \cdot \\ \cdot \\ A_m \end{bmatrix} \qquad \mathbf{\Pi} = \begin{bmatrix} \Pi_1 \\ \cdot \\ \cdot \\ \Pi_m \end{bmatrix} \tag{79}$$

In here, $\hat{\epsilon}$ and $\hat{\sigma}$ are diagonal matrices that take care of the material and geometrical weighting of the permittivity and conductivity.

$$\hat{\epsilon} = \begin{bmatrix} \epsilon_1 & \cdot & \cdot & \cdot & \cdot \\ \cdot & \epsilon_2 \cdot & \cdot & \cdot & \\ \cdot & \cdot & \cdot & \cdot & \cdot \\ \cdot & \cdot & \cdot & \cdot & \cdot \\ \cdot & \cdot & \cdot & \cdot & \epsilon_m \end{bmatrix} \qquad \hat{\sigma} = \begin{bmatrix} \sigma_1 & \cdot & \cdot & \cdot & \cdot \\ \cdot & \sigma_2 \cdot & \cdot & \cdot & \\ \cdot & \cdot & \cdot & \cdot & \cdot \\ \cdot & \cdot & \cdot & \cdot & \cdot \\ \cdot & \cdot & \cdot & \cdot & \sigma_m \end{bmatrix} \tag{80}$$

The matrix N represents the discretization of the operator $\nabla \times [1/\mu \nabla \times \ ] - 1/\mu \nabla [\nabla \cdot \ ]$ as described above. The matrix N is of size $m \times m$. The matrix M describes the coupling to the voltage degrees of freedom and is of size $m \times n$.

3.5 Boundary conditions for the Maxwell-Ampere equation.

First of all, we emphasize that there are two classes of boundary conditions. We already mentioned that the vector potential consists of *three* components (fields) and each component requires its own boundary condition. Just for convenience, suppose we have a domain boundary parallel to the (x,y)-plane. The Dirichlet boundary conditions are that the x and y component of the vector potential are vanishing at the boundary, i.e. $A_x = 0$ and $A_y = 0$. We still have two more fields to consider : the potential V and the 3rd component A_z. At the surface we should also respect the gauge condition. In particular, in the Lorentz gauge, we obtain at the surface that

$$\frac{1}{\mu}\frac{\partial A_z}{\partial z} + \epsilon \frac{\partial V}{\partial t} = 0 \tag{81}$$

Since the the tangential components of A vanish at the surface, and therefore also their partial derivatives with respect to x and y. The Dirichlet boundary condition for A_x and A_y physically corresponds to a magnetic field arriving tangential at the surface. This field is described by the curl of the z-component of $\mathbf{A}$, i.e.

$$B_x = \frac{\partial A_z}{\partial x} \qquad B_y = -\frac{A_z}{\partial y} \qquad B_z = \frac{\partial A_y}{\partial x} - \frac{\partial A_x}{\partial y} = 0 \tag{82}$$

This is just the magnetic field corresponding the a current impinging perpendicular at the surface. Such a field is needed since we can not carry a current to a contact without also impinging a magnetic field on that surface. So a good usage of the Dirichlet boundary condition is to use them for describing domain boundaries where contacts are found. Examples are pairs of contacts (ports) that are impinged by a TEM wave.

Contrary to Dirichlet boundary conditions, we also can imagine Neumann type of boundary conditions.

We look at a different class of boundary conditions for A_x and A_y. We will now invent something that resembles Neumann type boundary conditions for these fields. What could that be? Let us think of the surface parallel to the (x,y)-plane again. Now we want to say something about

$$\frac{\partial A_x}{\partial z} \qquad\qquad \frac{\partial A_y}{\partial z} \tag{83}$$

What can we say for these partial derivatives without using a primal link outside the simulation domain? Should we use links that by definition are not in the memory of the computer? No! We can say something about these partial derivatives.

$$\frac{\partial A_x}{\partial z} = -B_y = -\mathbf{B}\cdot\tau_y \qquad\qquad \frac{\partial A_y}{\partial z} = B_x = \mathbf{B}\cdot\tau_x \tag{84}$$

where τ is a tangential vector at the surface. For later use we define ν as a normal vector to the surface. So far, we did not achieve much. We substituted one piece of desired knowledge by another piece, since what to take for this $\mathbf{B}$? Here we may however apply some physics, Suppose that the boundary is located in some insulating region (air). Then we know that the solution satisfies the Maxwell equation in free space. Such solutions describe transverse polarized electromagnetic waves. *Asssuming* an outgoing wave perpendicular to the surface (in the z direction we can assert the value of these partial derivatives in terms of the link variables A_x and A_y themselves.

$$\mathbf{A}(\mathbf{x},t) = (A_x\mathbf{e}_x + A_y\mathbf{e}_y)\ \mathrm{e}^{j\omega t - jk_z z} \tag{85}$$

The plane TEM wave is characterized by a Dirichlet boundary condition on V, in particular $V=0$. Together with the gauge condition we find that $\mathbf{k}\cdot\mathbf{A}=0$, which explain (85). The wave satisfies

$$\left(\frac{1}{c^2}\frac{\partial^2}{\partial t^2} - \frac{\partial^2}{\partial z^2}\right)\mathbf{A} = 0 \tag{86}$$

In one dimension this is equivalent to

$$\left(\frac{1}{c}\frac{\partial}{\partial t} - \frac{\partial}{\partial z}\right)\left(\frac{1}{c}\frac{\partial}{\partial t} + \frac{\partial}{\partial z}\right)\mathbf{A} = 0 \tag{87}$$

For outgoing waves this boils down to

$$\left(\frac{1}{c}\frac{\partial}{\partial t} - \frac{\partial}{\partial z}\right)A_x = 0 \qquad\qquad \left(\frac{1}{c}\frac{\partial}{\partial t} - \frac{\partial}{\partial z}\right)A_y = 0 \tag{88}$$

This can be summarized as

$$\tau\cdot\mathbf{\Pi} = c\,(\nu\cdot\nabla)\tau\cdot\mathbf{A} \tag{89}$$

The Neumann boundary conditions for the surface links can be obtained from

$$\left(\frac{\partial}{\partial t} - c\,(\nu\cdot\nabla)\right)(\tau\cdot\mathbf{A}) = 0 \qquad\qquad \left(\frac{1}{c}\frac{\partial}{\partial t} - c\,(\nu\cdot\nabla)\right)(\tau\cdot\mathbf{\Pi}) = 0 \tag{90}$$

We will now present the detailed derivation of the matrices C and D. Our starting point will be the current-continuity equations for the contact nodes. The current continuity can be expressed as :

$$\nabla \cdot \mathbf{J} = 0 \quad \text{where} \quad \mathbf{J} = \mathbf{J}_{\text{cond}} + \mathbf{J}_{\text{disp}} \tag{91}$$

For a contact node the discrete assembling gives

$$\sum_j \Delta S_{ij} J_{ij} + I_i^{\text{out}} = 0 \tag{92}$$

In fig. (3) this is illustrated.

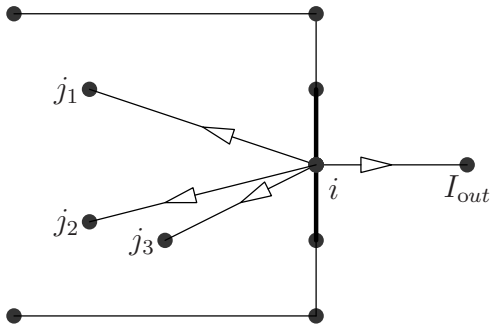

Figure 3: Illustration of the currents at a contact node, i. The nodes j are field nodes.

The total current for the contact is obtained by summing over all the contact nodes :

$$I^{\text{out}} = \sum_i I_i^{\text{out}} \tag{93}$$

The assembling of the current-continuity equations for internal nodes, j, runs over all links that are connected to j, including the contact nodes i. Whereas in the stand-alone field solving approach these contributions are not considered for the matrix building, we can evaluate these contributions for the construction of the matrices C and D. Using the fact that $J_{ij} = -J_{ji}$, the assembling leads to the following result :

$$\begin{aligned} -\sum_j \frac{\Delta S_{ij}}{h_{ij}} \sigma V_j + \sum_j \frac{\Delta S_{ij}}{h_{ij}} \sigma V_i + \sum_j \Delta S_{ij} \sigma \sigma_{ij} \frac{\mathrm{d}}{\mathrm{d}t} A_{ji} \\ - \sum_j \frac{\Delta S_{ij}}{h_{ij}} \frac{\mathrm{d}}{\mathrm{d}t} \epsilon V_j + \sum_j \frac{\Delta S_{ij}}{h_{ij}} \frac{\mathrm{d}}{\mathrm{d}t} \epsilon V_i \\ + \sum_j \Delta S_{ij} \epsilon \sigma_{ij} \frac{\mathrm{d}^2}{\mathrm{d}t^2} A_{ji} + I_i^{\text{out}} = 0 \end{aligned} \tag{94}$$

3.6 Time discretization

After space discretization, the coupled circuit-EM sytem can be written as differential-algebraic system of the form

$$f(\frac{\mathsf{d}}{\mathsf{d}t} q(x,t), x, t) = 0.$$

The most effective way to do a time integration of such systems in the curcuit world is known to be the backward differential formula (BDF) method. Applying the k-step BDF method yields

the nonlinear equation systems

$$f(\sum_{i=0}^{k} q(x_{n-i}, t_{n-i}), x_n, t_n) = 0.$$

for calculating x_n which approximates the solution point $x(t_n)$. The nonlinear equations are solved by Newtons method.

3.6.1 Time integration solvers

The first time integration solver for DAEs established here for the circuit-EM coupling uses the BDF methods and bases on the MATLAB DAE solver daen by Michael Hanke [9]. Here, it was adapted to the coupled problems and transferred to Python. It allows the solution of DAEs of the form

$$M(t)x' + f(x,t) = 0.$$

M can be constant or time dependent, but should not depend on x. For stability reasons, this form is not recommended for solving circuits with time-dependent or non-linear dynamic components. Therefore, a Python implementation of a BDF solver called bdfdae for solving DAEs of the form

$$f(\frac{\mathrm{d}}{\mathrm{d}t}q(x,t), x, t) = 0$$

has been developped. It includes an error controlled order and stepsize strategy. It allows a coupled circuit-EM simulation of nonlinear circuit models with nonlinear EM models via the nonlinear EM-circuit interface.

3.6.2 Python Code Design

We present briefly the basic files of the numcgnpy-package. For the time integration solver the following files are needed:

csparse.py	This file contains the main sparse matrix class Csparse.
exampledaes.py	All the example DAEs are given here as hard defined functions. They are organized in classes.
func.py	This file contains the classes Func and MFunc.
funcDAE_standard.py	In the class FuncDAE_standard the interface of a DAE with a DAE solver is specified. This is the main interface class for the different DAE formulations.
daen.py	This file contains the DAEn class which represents the DAEn solver.

4 Conclusions

This document describes the mathematical details and subtleties in order to successfully perform transient and coupled circuit-field solver approaches. The key concern is to end up after

discretization with a non-singular problem such that the linear solvers are confronted with a well-defined problem. Moreover, the discretization should respect basic physical requirement such as for example charge conservation. Our discretization scheme respects these requirements. Having a well-defined problem from the (mathematical perspective) provides an answer in a finite run time, but not necessarily the $correct$ answer. For that purpose it is needed that a sufficient amount of structural detail is included. In practice it requires that the computational mesh is fine enough to capture the relevant details.

References

[1] Codestar website. http://www.imec.be/codestar/.

[2] Cmos backbone for 2010 e-europe, nanocmos, from the 45nm node down to the limits. IST-Proposal, 2003.

[3] G. Alì, A. Bartel, M. Günther, and C. Tischendorf. Elliptic partial differential-algebraic multiphysics models in electrical network design. *Math. Models Meth. Appl. Sci.*, 13(9):1261 – 1278, 2003.

[4] Richard Barrett, Michael Berry, Tony F. Chan, James Demmel, June M. Donato, Jack Dongarra, Victor Eijkhout, Roldan Pozo, Charles Romine, and Henk Van der Vorst. *Templates for the Solution of Linear Systems: Building Blocks for Iterative Methods*. SIAM, 1994. http://www.netlib.org/templates/Templates.html.

[5] M. Bodestedt and C. Tischendorf. PDAE models of integrated circuits and index analysis. *Math. Comput. Model. Dyn. Syst.*, 13(1):1–17, 2007.

[6] M. Clemens, S. Drobny, H. Kruger, P. Pinder, O. Podebrad, B. Schillinger, B. Trapp, T. Weiland, M. Wilke, M. Bartsch, U. Becker, and M. Zhang. The electromagnetic simulation software package mafia 4. In *Computational Electromagnetics and Its Applications, 1999. Proceedings.*, pages 565–568, 1999.

[7] Bart Denecker. *De subdomein FDTD methode*. PhD thesis, Universiteit Gent, 2003.

[8] D. Estévez Schwarz and C. Tischendorf. Structural analysis of electric circuits and consequences for MNA. *Int. J. Circ. Theor. Appl.*, 28:131–162, 2000.

[9] M. Hanke. A new implementation of a bdf method within the method of lines. Technical report, Report No. 2001:01, Royal Institute of Technology, Stockholm, 2001.

[10] I. Higueras, R. März, and C. Tischendorf. Stability preserving integeration of index-1 DAEs. *APNUM*, 45:175–200, 2003.

[11] I. Higueras, R. März, and C. Tischendorf. Stability preserving integeration of index-2 DAEs. *APNUM*, 45:201–229, 2003.

[12] Snezana Jenei. *Characterization and optimization of the RF performances of analog components in CMOS and BiCMOS*. PhD thesis, KUL-IMEC, 2003.

[13] Domenico Lahaye. *Algebraic multigrid for two-dimensional time-harmonic magnetic field computations*. PhD thesis, KUL, 2001.

[14] S.E. Laux. Techniques for small-signal analysis of semiconductor devices. *IEEE Trans. Computer-Aided Design*, 4(10):472–481, 1985.

[15] Wil Schilders and Jan Ter Maten (Eds). *Handbook of Numerical Analysis : Numerical Methods in Electromagnetism*. Elsevier Publishing Company, the Netherlands, 2003.

[16] Wim Schoenmaker, Wim Magnus, and Peter Meuris. Strategy for electromagnetic interconnect modeling. *IEEE Trans. on CAD*, 20:753–762, 2001.

[17] Wim Schoenmaker, Wim Magnus, and Peter Meuris. Ghost fields in classical gauge theories. *Phys. Rev. Lett*, 88(18):181602–1 – 181602–4, 2002.

[18] Wim Schoenmaker, Wim Magnus, Peter Meuris, and Bert Maleszka. Renormalization group meshes and the discretization of tcad equations. *IEEE Trans. on CAD*, 21(12):1425–1433, 2002.

[19] Wim Schoenmaker and Peter Meuris. Electromagnetic interconnects and passives modeling: Software implementation issues. *IEEE Trans. on CAD*, 21:534–543, 2002.

[20] Sebastian Schöps. Coupling and simulation of lumped electric circuits refined by 3-D magnetoquasistatic conductor models using MNA and FIT. Master's thesis, Bergische Universität Wuppertal, 2008.

[21] Monica Selva Soto and Caren Tischendorf. Numerical analysis of DAEs from coupled circuit and semiconductor simulation. *Appl. Numer. Math.*, 53(2-4):471–488, 2005.

[22] A. Sidi. Efficient implementation of minimal polynomial and reduced rank extrapolation methods. *J. Comput. Appl. Math.*, 36:305–337, 1991.

[23] J. Stoer and R. Bulirsch. *Introduction to Numerical Analysis, 2nd ed.* New York: Springer-Verlag, 1993.

[24] Caren Tischendorf. *Coupled Systems of Differential Algebraic and Partial Differential Equations in Circuit and Device Simulation. Modeling and Numerical Analysis*. 2004. Habilitation thesis at Humboldt Univ. of Berlin.

[25] K. Yee. Numerical solution of initial boundary value problems involving maxwell's equation in isotropic media. *IEEE Trans. on Antennas and Propagation*, AP-14:302–307, 1966.